PERGAMON

Journal of Atmospheric and Solar-Terrestrial Physics 65 (2003) 583–590

Journal of ATMOSPHERIC AND SOLAR-TERRESTRIAL PHYSICS

www.elsevier.com/locate/jastp

# $N_2(B^3\Pi_g)$ and $N_2^+(A^2\Pi_u)$ vibrational distributions observed in sprites

E. Bucsela[a,*], J. Morrill[b], M. Heavner[c], C. Siefring[d], S. Berg[e], D. Hampton[f], D. Moudry[g], E. Wescott[g], D. Sentman[g]

[a] *Goddard Earth Science and Technology Center, Baltimore, MD, USA*
[b] *E.O. Hulburt Center for Space Research, Naval Research Laboratory, Washington, DC, USA*
[c] *Los Alamos National Laboratory, Los Alamos, NM, USA*
[d] *Plasma Physics Division, Naval Research Laboratory, Washington DC, USA*
[e] *Computational Physics Inc., Springfield, VA, USA*
[f] *Ball Aerospace & Technology Corp., Boulder, CO, USA*
[g] *Geophysical Institute, University of Alaska Fairbanks, Fairbanks, AL, USA*

**Abstract**

A pair of spectra taken simultaneously by two different ground-based instruments has been analyzed by our group. As with previous observations, the spectra are composed primarily of the $N_2$ first positive group (1PG) ($B^3\Pi_g - A^3\Sigma_u^+$). In a previous study, we compared the $N_2(B)$ vibrational distributions from the spectral analysis with those resulting from a time-dependent kinetic model of $N_2$ triplet excited state populations. Both spectra reflect emission between 50 and 60 km. The higher-altitude spectrum is primarily 1PG but also shows the presence of features which appear to be $N_2^+$ Meinel ($A^2\Pi_u - X^2\Sigma_g^+$). The lower-altitude spectrum shows little or none of the apparent Meinel emission but has an $N_2(B)$ vibrational distribution similar to ones observed in laboratory afterglows. In this paper we discuss the apparent presence of the Meinel emission and present the observed $N_2(B)$ vibrational distributions.


*Keywords:* Red sprites; Ionized $N_2$; 1PG and Meinel spectra; Vibrational distributions

## 1. Introduction

Since the earliest reports of red sprites appeared in the scientific literature (Franz et al., 1990; Sentman and Wescott, 1993; Lyons, 1994), the publication of new image and spectral observations of this phenomenon has continued at a rapid pace. Observations during the summer of 1995 (Mende et al., 1995; Hampton et al., 1996) were the first set of spectral measurements of sprites. These studies showed the predominant red emission to be produced by the $N_2$ first positive group (1PG) ($B^3\Pi_g - A^3\Sigma_u^+$). Recently, the UV/blue spectrum of sprites at ~65 km has been reported by Heavner et al. (2000) and Siefring et al. (1997), and this also appears to consist primarily of emission from neutral species, namely the $N_2$ second positive group (2PG) ($C^3\Pi_u - B^3\Pi_g$).

An important issue in sprite studies has been the determination of electron energies needed to produce the observed spectra. The dominance of neutral emissions in the early red observations implied that highly energetic processes were not required to generate sprites (Mende et al., 1995; Hampton et al., 1996). These findings were supported in subsequent spectral analysis by Green et al. (1996) and Milikh et al. (1998) using steady-state models to estimate the associated electron energies. However, additional photometric (Armstrong et al., 1998, 2000; Suszcynsky et al., 1998) and imaging (Morrill et al., 2002) observations at UV and blue wavelengths revealed both neutral $N_2$ emissions (2PG) and

* Corresponding author. Tel.: +1-301-614-6003; fax: +1-301-614-5903.
*E-mail address:* bucsela@hyperion.gsfc.nasa.gov (E. Bucsela).

1364-6826/03/$ - see front matter © 2003 Elsevier Science Ltd. All rights reserved.
doi:10.1016/S1364-6826(02)00316-4

ionized emissions from the first negative group (1NG) ($B^2\Sigma_g - X^2\Sigma_u^+$) of $N_2^+$. These measurements have confirmed the presence of $N_2^+$ in sprites. The results are significant, because the threshold energies needed for ionized emissions are on the order of 10 eV higher than those required for excitation of neutral emissions. Morrill et al. (2002) estimated characteristic electron energies and electric fields associated with the UV/blue observations between 45 and 70 km. Interpretation of the data has also been aided by numerous model calculations from Pasko et al. (1995, 1997), Fernsler and Rowland (1996), and Rowland (1998) that predict densities of electrons and emissions from excited $N_2$ states over a range of altitudes.

Further evidence of ionization in sprites may be provided by the $N_2^+$ Meinel bands. The $N_2^+(A)$ state has a longer lifetime (~10 μs) than the $N_2^+(B)$ state (~60 ns) and so tends to be more susceptible to quenching. However, Meinel bands may be seen if quenching is not too strong and $N_2^+$ production is significant. $N_2^+$ Meinel quenching coefficients have been presented by Piper et al. (1985) but, as they discuss, other energy transfer processes beyond simple quenching do occur. As a result, the presence of $N_2^+$ Meinel may reflect these processes during the ionization phase in sprites. Green et al. (1996) estimated upper limits for the Meinel emissions but indicated that these were at the noise level. Meinel emission in the near infrared is indicated in the analysis by Morrill et al. (1998). Confirmation of the presence and altitude dependence of Meinel bands would add support to studies indicating the production of ionized nitrogen in sprites.

Here we re-examine the findings of Morrill et al. (1998) and compare them with analysis of another spectrum from the same sprite. The two observations differ in both altitude and azimuthal position, with one measured at 53 km and the other at 57 km. Both are spectra from the tendril region of the sprite. Analysis shows that the spectra differ in the relative intensities of emission features. In their study, Morrill et al. (1998) calculated model distributions of $N_2$ excited states using a time-dependent kinetic model and compared them to the $N_2(B)$ distribution derived from the 57 km spectrum. That study concluded that a portion of the spectrum near 8000 Å did appear to be $N_2^+$ Meinel emission and could not be explained by $N_2$ 1PG emission alone. The spectral analysis that supports this conclusion was not presented in that study and will be discussed here in detail. In addition to the $N_2^+$ Meinel, we examine a number of other possible emissions that could be responsible for the 8000 Å spectral feature.

We also present analysis of a spectrum from 53 km. This spectrum is from a brighter region that is nearer the center of the tendrils. The spectrum shows little or no emission associated with $N_2^+$ Meinel. However, it does yield an $N_2(B)$ vibrational distribution that differs somewhat from that of the 57 km spectrum. The observed distribution from this region of the sprite appears similar to ones observed in laboratory $N_2$ afterglows. The mechanism that is known to yield the laboratory results and its possible relevance to sprites will be discussed.

## 2. Observations

The sprite under examination occurred at 03:58:24 UT on 24 July 1996. Spectra were taken by two spectrographs of different resolutions, which were coaligned with a pair of visible imagers differing in field-of-view (FOV) and wavelength sensitivity. The simultaneous images allowed the spectrographic data to be correlated with the physical features of the sprites and provided information about the viewing geometry.

Fig. 1 shows a portion of the image from the wider-field camera whose full FOV measures 15° horizontally ×10° vertically. It was captured using an intensified CCD system with a response that is broad at optical wavelengths, but most sensitive in the red. A second imager viewed an area of the sky 12.2 × 7.8° and observed only the right portion of this sprite. This small FOV camera is slightly more sensitive at the blue end of the visible spectrum with a cutoff in response below ~4000 Å. Horizontal lines in Fig. 1 mark the projections of the slits from the two spectrographs. The dashed line corresponds to the high resolution (70 Å FWHM) "Deehr" TV spectrograph, which focuses the sky onto a slit using an $f/0.7$ lens. Light from the slit is collimated and dispersed by a grating before being imaged onto an intensified CCD detector. More information on the Deehr TV spectrograph


Fig. 1. Image of sprite observed at 03:58 UT on 24 July 1996. Also shown are the slits of the two spectrographs overlaid on the sprite image. The lower, dashed, horizontal line is the projection of the high-resolution (70 Å) spectrograph at 53 km. The upper, solid horizontal line shows the projection of the low-resolution (~110 Å) spectrograph at 57 km.

is given by Hallinan et al. (1985) and Hampton et al. (1996). Also in Fig. 1, the higher, solid horizontal line is the slit position of the "Fogel" spectrograph, which has a resolution between 90 and 130 Å in the spectral range analyzed here. A sprite spectrum from the Fogel spectrograph has been presented by Morrill et al. (1998). The Fogel spectrograph uses a 50 mm $f/1.2$ lens that focuses on an entrance slit. Light is then collimated with a similar lens, passed through a grating and re-focused onto an intensified CCD. For the measurements made on 24 July 1996, both instruments viewed a spectral range that included red and near infrared wavelengths. The sensitivities of the two spectrographs were determined from laboratory and field calibrations.

The time and location of the observations were obtained from ancillary sources. All of the systems were sync-locked with a GPS timing system, which is limited by the video field rate to a temporal resolution of 17 ms. The projected altitudes of the spectrograph slits were determined by the location of the associated lightning and our knowledge of sprite morphology. For the sprite observation considered in this study, the observing altitude of the low-resolution Fogel spectrograph was found to be $57 \pm 2$ km, and that of the high-resolution Deehr TV spectrograph was $53 \pm 1$ km.

## 3. Spectral analysis and results

The two sprite spectra were analyzed by similar methods. A description of the method used to extract the components of the higher-altitude spectrum has been presented by Morrill et al. (1998). We will review the procedure here and present further details about the analysis of both spectra. The focus of this section is the $N_2$ 1PG and $N_2^+$ Meinel emissions. We have also considered a number of other possible sources of the observed emission near 8000 Å, and this analysis is presented in the following section.

Synthetic spectral features were generated for fitting to the data. The features included progressions of the $N_2$ 1PG system with upper vibrational levels $v' = 1$–8, as well as the two $N_2^+$ Meinel progressions originating from the $v' = 2$ and 3 levels. Rotational lines were computed at a temperature of 230 K by a band-synthesis algorithm (Bucsela and Sharp, 1997), and as noted by Morrill et al. (1998), the fit is relatively insensitive to rotational temperature at the instrument's course spectral resolution. The resulting theoretical intensities were attenuated by wavelength-dependent atmospheric absorption factors from the MOSART radiative transfer model (Corenette et al., 1994). Absorption factors were based on an assumed sprite altitude of 55 km and an observation path length of 520 km. The attenuated spectra were convolved with Gaussian instrument functions that were found to best fit the features of each spectrum. The low-altitude, high-resolution spectrum had a FWHM resolution of approximately 70 Å across the entire analyzed range of 6190–8970 Å. The high-altitude spectrum, discussed by Morrill et al. (1998), had an instrument function characterized by a Gaussian with a variable FWHM that ranged from 90 Å at 6200 Å to 130 Å at 9000 Å.

The two spectra were each fitted with 24 molecular bands (21 1PG and 3 Meinel) from the 10 upper vibrational levels of the two systems. Data weights for the chi-square minimization routine were based on an estimate of the noise level at each wavelength as determined from the variability of the signal over intervals smaller than a wavelength resolution element. As the noise level was higher in both spectra at longer wavelengths, the shorter wavelengths were weighted more heavily in the fits. A small linear compression of the wavelength scale amounting to less than 80 Å was introduced across the spectral range to improve the fits of the two brightest 1PG bands. The uncertainty in the wavelength scale at any point is approximately $\pm 30$ Å, and a number of deviations between the fit and the observation can be seen in the results.

In addition to the 10 molecular band progressions, each spectrum was fitted with and without a uniform background whose amplitude was varied with the molecular features as an additional fitting parameter. However, the resulting amplitude of the fitted background was small, and the fitted amplitudes of the brightest molecular bands were relatively insensitive to whether the background was present or not. Inclusion of the background reduced the 1PG $v' = 1$–5 progressions and the Meinel $v' = 2$ progression by no more than 10% in the high-altitude spectrum and 5% in the low-altitude spectrum. Results of the two spectral fits with the background removed are shown in Figs. 2 and 3, along with the corresponding vibrational distributions.

The lower-altitude spectrum (Fig. 2a) was taken near the center of the tendril portion of the sprite and shows little or no Meinel emission. The $N_2(B)$ distribution appears in Fig. 2b. This distribution is very similar to the $N_2(B)$ afterglow distribution observed elsewhere (Piper, 1989; Morrill and Benesch, 1996) and is reproduced in Fig. 4. The fit to the higher-altitude spectrum appears in Fig. 3. Note that the "1PG & Meinel" vibrational distributions (Fig. 3d) resulting from the high-altitude fit (Fig. 3a) are essentially the same as those plotted in Fig. 2 of Morrill et al. (1998), in which a small, fixed (not fitted) background was assumed.

An important difference between the 57 km and the 53 km spectra is the apparent presence of $N_2^+$ Meinel band emissions in the higher-altitude spectrum between 7800 and 8200 Å (Fig. 3). The magnitude of these features is only marginally significant in the 53 km spectrum, as shown by the error bars in the derived vibrational population in Fig. 2b. We investigated the possibility that the apparent Meinel emission seen in the higher-altitude spectrum might be 1PG emission, primarily the 1PG (7,6) band, which emits in the same region. This investigation was briefly mentioned by Morrill et al. (1998) and is illustrated here in more detail. Figs. 3b and c show two alternative fits to the 57 km spectrum, both with Meinel emission removed from the fit. In one fitting scenario (Fig. 3b), the entire 6200–9000 Å range was fitted, and results show that the model was

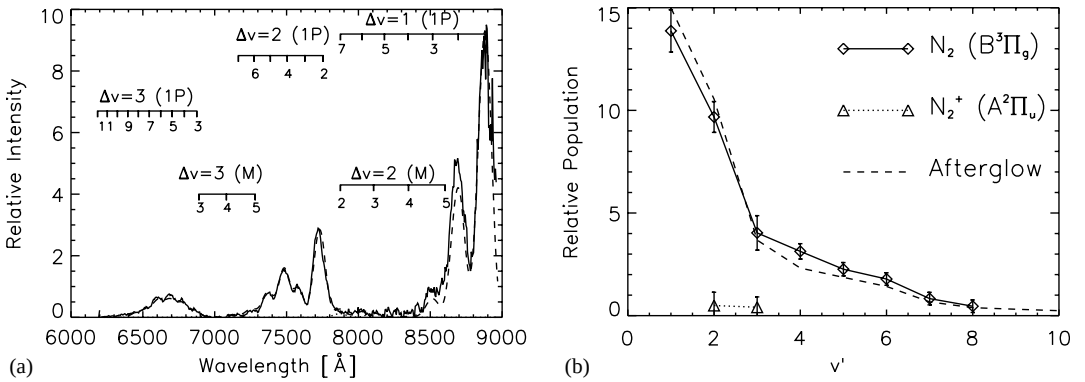


Fig. 2. (a) Calibrated 53 km sprite spectrum (—-) recorded by the high-resolution spectrograph and the synthetic fit (- - -). Band labels are shown above the spectrum. The $N_2^+$ Meinel emission (....) near 7900 Å is negligible. (b) Derived vibrational populations for the upper states of the $N_2$ 1PG (—-) and $N_2^+$ Meinel bands (....). A laboratory afterglow distribution (- - -) is also shown.

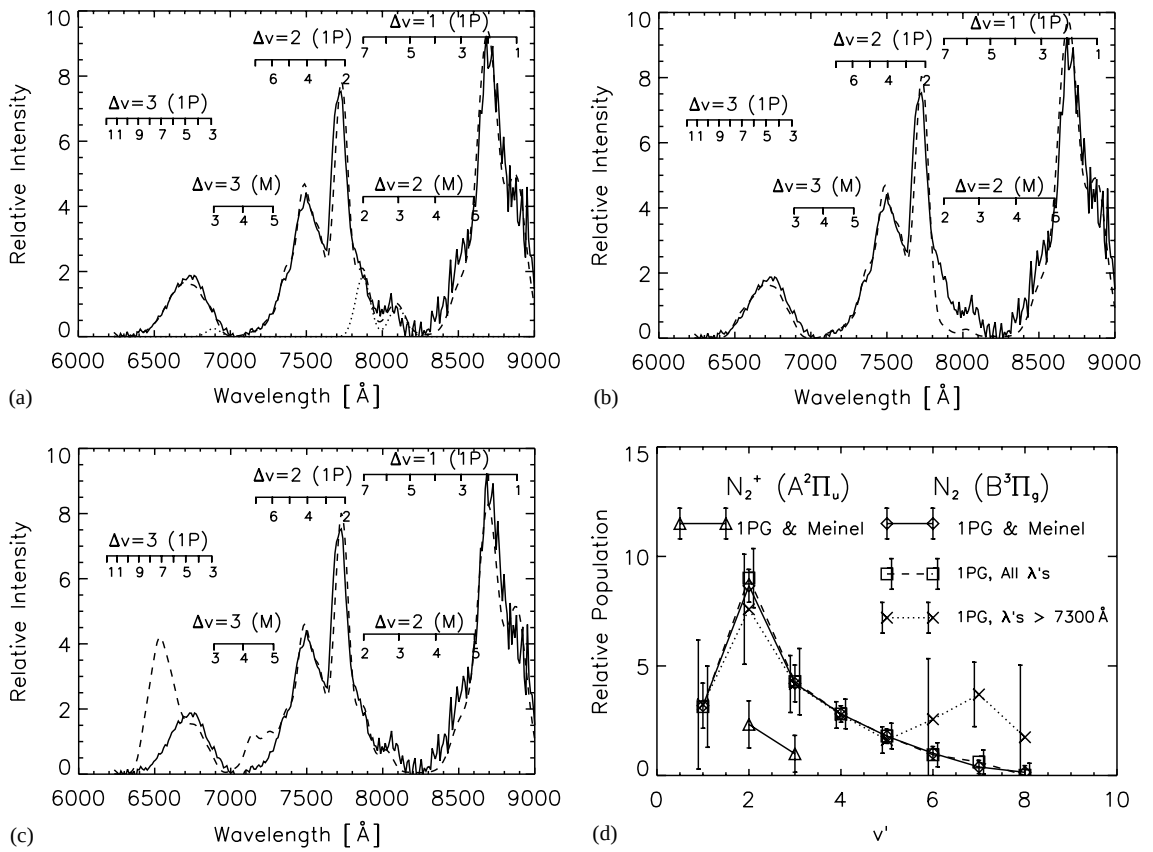


Fig. 3. (a) Calibrated 57 km sprite spectrum (—) recorded by the low-resolution spectrograph and the synthetic fit (- - -). Band labels are shown above the spectrum. $N_2^+$ Meinel emission (....) can be seen near 7900 Å. (b) Same as (a), but spectrum was fitted without Meinel bands. (c) Same as (b), but only wavelengths greater than 7300 Å were fitted. (d) Derived vibrational populations of the $N_2$ 1PG and $N_2^+$ Meinel bands from spectral fits (a)–(c).

unable to reproduce the emission in the observed spectrum near 8000 Å when using 1PG alone. In another scenario (Fig. 3c), only wavelengths longer than 7300 Å were fitted. The excess model emission near 6500 Å is primarily the 1PG (7,4) band, which appears large due to the algorithm's attempt to fill the 8000 Å data with the 1PG (7,6) band. The unreasonable enhancement of the $v' = 7$ level, as well as the adjacent $v' = 6, 8$ levels, can be seen in the

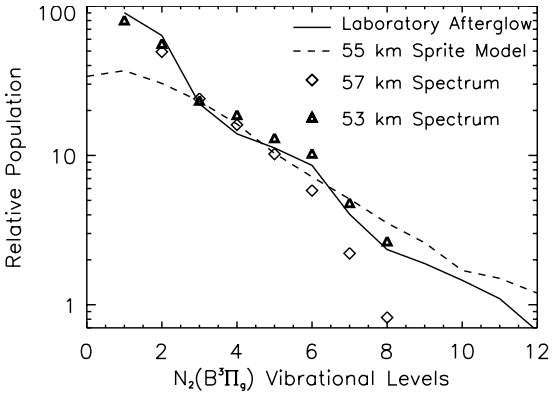


Fig. 4. $N_2$(B) vibrational distributions from spectrum 2a (▲) and 3a (◇), compared with a laboratory afterglow (—-), and a sprite model at 55 km (- - -).

resulting vibrational distribution shown in Fig. 3d. These figures demonstrate the fact that the observed intensity near 8000 Å cannot be due to 1PG emission and that Meinel emission is a probable cause. In the next section we discuss other known spectral emissions in this wavelength region produced by species present in the atmosphere.

A second difference between the two spectra is evident in the lower-vibrational levels of the $N_2(B)$ state. As Fig. 3d illustrates, the population of the $v' = 1$ level is suppressed relative to the $v' = 2$ level in the 57 km spectrum. While some of this effect may have a geophysical basis, a more likely explanation is that an error in the instrument sensitivity calibration exists above 8500 Å, where the 1PG (1,0) band is located. The calibration of the spectrograph used to record the 53 km spectrum (Fig. 2a) is more certain in the same spectral region, and the resulting data do not show the same anomaly in the $v' = 1$ level.

## 4. Other possible emissions near 8000 Å

We have considered four additional band systems as alternative sources of the apparent Meinel emission. These are the $O_2$ red atmospheric system, the $N_2$ infra-red afterglow (IRA) system, and nitric oxide emissions from the infra-red quartet system and Ogawa's *b*-system. The following is an examination of these systems and the difficulties they present in accounting for the observed sprite emission near 8000 Å.

The $O_2$ red atmospheric system ($b^1\Sigma_g^+ - X^3\Sigma_g^-$) is a dipole-forbidden transition, although it is a significant absorber near 7620 Å. Here, we investigate the possibility that the emission near 8000 Å is actually due to the $O_2$ atmospheric (3,3) band at 7904 Å. A simple calculation reveals that the intensity of this band in the sprite spectrum should be negligible relative to the $N_2$ first positive system. The $O_2(b)/N_2(B)$ population ratio can be estimated using the relative excitation rates of Morrill et al. (2002) and quenching rates at 55 km of ~99% for the $O_2(b)$ state (R. Copeland, Private Communication) and ~50% for the $N_2(B)$ state (based on simple quenching). This yields an anticipated excited state population ratio of ~0.04. Scaling the $O_2(b)$ population with the $O_2(b-X)$ (3,0) Franck–Condon factor (assuming electron impact production of $O_2(b)$) and the $N_2(B)$ population with a factor derived from an estimate of the relative population of the $N_2(B, v=2)$ population from the 1PG spectrum, we get an $O_2(b, v=3)/N_2(B, v=2)$ population ratio of $\sim 1.1 \times 10^{-5}$. Further scaling this value by the appropriate transition probabilities for the first positive and atmospheric band systems (Krupenie, 1972) gives an estimated intensity ratio of $\sim 1.2 \times 10^{-11}$ for the $O_2(b-X)(3,3)$ band relative to the $N_2(B-A)(2,0)$ band. This ratio is far smaller than the observed ratio (~0.2) between the intensities of the emission near 8000 Å and the $N_2(B-A)(2,0)$ band emission in the sprite spectrum. Therefore, it is highly unlikely that the $O_2$ atmospheric (3,3) band is the source of the enhanced sprite emission near 8000 Å.

The (4,0) and (8,3) bands of the $N_2$ infra-red afterglow system ($B'^3\Sigma_u^- - B^3\Pi_g$) also emit in the vicinity of 8000 Å. We can predict populations for the upper vibrational levels of these bands relative to upper levels of the $N_2(B-A)$ system. The ratios may then be compared to ratios derived from the sprite spectrum under the assumption that the IRA bands are responsible for the 8000 Å emission. Benesch and Fraedrich (1984) found $N_2(B', v)$ populations to be in collisional equilibrium with those of $N_2(B, v+4)$, since these $B'$ and $B$ levels have nearly the same energy. The equilibrium is reflected in model- and laboratory-derived population ratios on the order of unity for $N_2(B', v=4)/N_2(B, v=8)$ and for $N_2(B', v=8)/N_2(B, v=12)$. Laboratory measurements by Benesch and Fraedrich (1984) yield values of 1.9 and 2.4, respectively, for these ratios, while our sprite model predicts corresponding values of 0.75 and 2.8 at 55 km. In contrast, the sprite spectrum would imply respective ratios of ~90 and ~270 if the 8000 Å emission were due to the IRA (4,0) and (8,3) bands. The fact that these ratios are two orders of magnitude larger than predictions casts doubt on the identity of the emission as IRA bands. Furthermore, no IRA observations in this wavelength region have been reported in previous airglow or auroral studies, whereas $N_2^+$ Meinel emission is common (Broadfoot et al., 1997).

Laboratory studies have detected weak nitric oxide (NO) emissions in the red and near-infrared spectral regions. A good review of these investigations is given by Pearse and Gaydon (1976). Only two reported systems have bands that emit near 8000 Å, namely Ogawa's *b*-system ($b - B^2\Pi$), and the infrared quartet system, which Brook and Kaplan (1954) attribute to a ($^4\Pi - {}^4\Pi$) transition. Each system includes one or two bands that overlap a portion of the 7800–8200 Å region, where the enhanced sprite emission is observed. However, laboratory spectra indicate that these systems also contain bands of comparable intensity not seen in the sprite data. For example, the (0,2) Ogawa-*b* band near 8020 Å should be accompanied by the (0,1), (0,0),

(1,0), and (2,2) bands near 7420, 6900, 6380, and 6750 Å, respectively. None of these emissions is evident in the sprite spectrum. Likewise, if the NO IR-quartet (2,0) and (3,1) bands between 7800 and 7930 Å were the source of the observed sprite emission, the stronger (1,0) and (2,1) bands between 8530 and 8730 Å should also be present. These latter bands are also absent in the data. Thus, the laboratory data imply that neither NO system alone or in combination could produce the observed emissions near 8000 Å without additional emissions in other parts of the spectrum.

## 5. Discussion

The preceding sections lend support to the conclusions of Morrill et al. (1998) that Meinel emission is present in the 57 km spectrum. However, as was stated, the presence of $N_2^+$ Meinel emission in sprites is controversial because the Meinel upper state, $N_2^+(A)$, is reported to be strongly quenched (Piper et al., 1985). Since the altitudes of both measurements are less than 60 km, thus well below the emission's reported quenching height of 85–90 km (Vallance Jones, 1974), any Meinel emission present in the spectra should be difficult to detect. However, as discussed by Piper et al. (1985), the work by Katayama et al. (1980) and Katayama (1984) shows that energy transfer between $N_2^+(A)$ and $N_2^+(X)$ is a rapid process and may play a role in the presence of $N_2^+$ Meinel emission in the sprite spectrum. Further examinations of existing and future visible and near-IR spectra are needed to confirm these results. Aircraft (Sentman et al., 1997 Morrill et al., 2002) and photometric (Armstrong et al., 1998, 2000; Suszcynsky et al., 1998) observations show emissions from the $N_2^+$ 1NG, indicating that $N_2^+$ excited states are indeed formed in sprites. The results of Morrill et al. (2002) show the relative $N_2^+$ UV/blue emissions to be brightest in the tendrils (below 55–60 km), where the present $N_2^+$ Meinel observations were obtained.

As we have shown, significant Meinel emission is evident only in the higher altitude spectrum. Since quenching affects the $N_2^+(A)$ state and this effect increases with decreasing altitude, the difference between the spectra appears consistent with the identification of the 7800–8200 Å emission as $N_2^+$ Meinel. However, the altitude separation of the spectra is small, and other effects may play a greater role. Fig. 1 shows that the 53 km spectrum is dominated by brighter emission near the center of the tendril region. In contrast, the 57 km spectrum includes weaker emission near the edge of a smaller tendril. If the brighter central region contains a disproportionate amount 1PG emission, any Meinel present in the 53 km spectrum may be masked by the brighter 1PG bands. We have also considered a number of other possible sources of the enhanced emission near 8000 Å but none of them present likely alternatives. However, more observations are needed to distinguish among these and other possibilities and to confirm the source of this emission in sprite spectra.

Fig. 4 shows the $N_2(B)$ vibrational distribution from both spectra in addition to a laboratory afterglow distribution (Morrill and Benesch, 1994) and a model sprite distribution for 55 km. Details of the model have been discussed by Morrill et al. (1998) and Morrill and Benesch (1996). The model results in Fig. 4 were computed using excitation rates at 55 km from the work of Morrill et al. (2002), and the narrow excitation pulse for the 75 km case of Morrill et al. (1998). Recent high-speed video observations (D. Moudry, Private Communication) support the assumption of short excitation pulses in sprite tendrils. Morrill and Benesch (1996) have shown that the model effectively reproduces auroral data when electron impact is the principal excitation mechanism. The afterglow distribution in Fig. 4 is indicative of an energy transfer process between vibrationally excited $N_2$ ground state and the lowest-energy, metastable electronic state (Piper, 1989; Morrill and Benesch, 1994). The reaction is

$$N_2(A) + N_2(X, v \geqslant 5) \rightarrow N_2(B) + N_2(X, v{\sim}0). \quad (1)$$

Radiative decay of the $N_2(B)$ state, in turn, produces the $N_2(A)$ state through 1PG emission so that $N_2(A)$ acts as a catalyst in this reaction. The process has been the subject of a number of studies (Piper, 1989; Morrill and Benesch, 1994) and can be an important source of $N_2(B)$ in environments where vibrationally excited $N_2(X)$ is a dominant specie (Picard et al., 1997).

Some inference about possible excitation mechanisms in sprites may be drawn from Fig. 4. The 55 km sprite model used to produce the model distribution in Fig. 4 contains only direct excitation by electron impact, radiative cascade, quenching, and collisional transfer between the $N_2(B)$ and other nearby triplet states. Processes like Eq. (1) are not incorporated in the present version of the model. As seen in the figure, the model (dashed line) is a poor representation of the distribution from either the 53 or 57 km sprite spectrum. On the other hand, the afterglow distribution (solid line) closely resembles the 53 km distribution, as well as the low-$v$ portion of the 57 km distribution. The high-$v$ distribution from the 57 km spectrum does not resemble either the afterglow or the sprite-model distribution. Although relative uncertainties in the high-$v$ levels of the 57 km spectrum are larger than those of the 53 km spectrum, some of the discrepancy might also result from deficiencies in the sprite model. These may include overestimation of collisional transfer, or the failure of the model to include Eq. (1). Nonetheless, the low-level vibrational distributions from both spectra clearly imply that processes beyond simple electron impact are active during sprite excitation.

The afterglow reaction (Eq. (1)) can contribute significantly to the observed $N_2(B)$ vibrational distribution only if its rate is appreciable relative to that of other $B$-state sources. Since electrons with sufficient energy to ionize $N_2$ are present, it is likely that electron impact is responsible for a portion of the $N_2(B)$ produced. The relative afterglow contribution then depends on the rate coefficient of Eq. (1)

(measured by Piper (1989)) and the local amounts of $N_2(A)$ and vibrationally excited $N_2(X)$. Both species are the product of electron-impact excitation, with a significant fraction of the lower vibrational levels of the A-state populated by cascade from other $N_2$ triplet electronic states (Cartright, 1978; Morrill and Benesch, 1996). Although no direct measure of the $N_2(A)$ populations have been made, Morrill et al. (1998) show that the populations can be estimated using the electrostatic heating model of Pasko et al. (1997). A comprehensive treatment of sprite excitation would need to include other species such as $O_2$ and $CO_2$, as they are likely to play a significant role in energy transfer processes. The present results are not adequate to assign Eq. (1) as the major source of the observed 1PG spectrum. However, the observed $N_2(B)$ vibrational distribution is strongly suggestive of this mechanism.

## 6. Summary and conclusions

The data and analysis presented here add to the growing body of information about excitation processes in sprites. We have analyzed two spectra from different regions of the same sprite. The higher altitude spectrum shows evidence of $N_2^+$ Meinel bands. This observation along with other studies (e.g., Morrill et al., 2002) imply the presence of electron energies sufficient to produce $N_2^+$ in sprites. The absence of Meinel emission in the lower altitude spectrum may result from increased quenching or from other causes. Additional spectra obtained at a variety of altitudes, at wavelengths from the UV to the near-infrared, and with improved temporal resolution, are needed to understand the distribution of $N_2$ and $N_2^+$ excited states. Such data would be valuable, particularly in light of the questions regarding quenching of the Meinel emission.

At lower altitudes, where gas densities are greater, the $N_2(B)$ vibrational distribution derived from this study suggests that a less energetic process, like that seen in laboratory afterglow spectra, plays a role in the observed 1PG emission. The similarity to afterglows implies that some sprite emission is produced by collisional processes involving vibrationally excited $N_2$. Additional observation are needed to confirm this hypothesis. Such studies could shed further light on the detailed ionization and excitation processes occurring in sprites and related phenomena.

## Acknowledgements

The computer time was supported in part by the Solar Physics and X-Ray Branches of the Space Science Division (SSD) of the Naval Research Laboratory (NRL), with additional computer time provided by NASA Goddard Space Flight Center. The atmospheric transmission calculations were performed using the MOSART model as implemented in the SSGM (Synthetic Scene Generation Model) at the SSD/NRL. E. Bucsela was supported by an ASEE Postdoctoral Fellowship. J. Morrill was supported in part by the Edison Memorial graduate training program at NRL. D. Moudry, M. Heavner, D. Hamptom, D. Sentman, and E. Wescott were supported by NASA Grant NAG5-5019. We thank the referees for their very useful comments and suggestions.

## References

Armstrong, R., Shorter, J., Taylor, M., Susczynsky, D., Lyons, W., Jeong, L., 1998. Photometric measurements in the SPRITES 1995 and 1995 campaigns. Journal of Atmospheric and Solar-Terrestrial Physics 60, 787–799.

Armstrong, R., Susczynsky, D., Lyons, W., Nelson, T., 2000. Multi-color photometric measurements of ionization and energy in sprites. Geophysical Research Letters 27, 653–656.

Benesch, W., Fraedrich, D., 1984. The role of intersystem collisional transfer of excitation in the determination of $N_2$ vibronic level populations. Journal of Chemical Physics 81, 5367–5374.

Broadfoot, A., Hatfield, D., Anderson, E., Stone, T., Sandel, B., Gardner, J., Murad, E., Knecht, D., Pike, C., Viereck, R., 1997. $N_2$ triplet band systems and atomic oxygen in the dayglow. Journal of Geophysical Research 102, 11567–11584.

Brook, M., Kaplan, J., 1954. Dissociation energy of NO and $N_2*$. Physical Review 96, 1540–1542.

Bucsela, E.J., Sharp, W.E., 1997. NI 8680 and 8629 Å multiplets in the dayglow. Journal of Geophysical Research 102, 2457–2466.

Cartright, D.C., 1978. Vibrational populations of the excited states of $N_2$ under auroral conditions. Journal of Geophysical Research 83, 517–531.

Corenette, W.M., Acharya, P.K., Anderson, G.P., 1994. Using the MOSART code for atmospheric correction. IEEE Conference Proceedings on International Geoscience and Remote Sensing Symposium, Pasadena, CA, Vol. 1, pp. 215–219.

Fernsler, R., Rowland, H., 1996. Models of lightning-produced sprites and elves. Journal of Geophysical Research 101, 29653–29662.

Franz, R.C., Nemzek, R.J., Winckler, J.R., 1990. Television image of a large upward electrical discharge above a thunderstorm system. Science 249, 48–51.

Green, B.D., Fraser, M.E., Rawlins, W.T., Jeong, L., Blumberg, W.A.M., Mende, S.B., Swenson, G.R., Hampton, D.L., Wescott, E.M., Sentman, D.D., 1996. Molecular excitation in sprites. Geophysical Research Letters 23, 2161–2164.

Hallinan, T.J., Stenbaek-Nielsen, H.C., Deehr, C.S., 1985. Enhanced aurora. Journal of Geophysical Research 90, 8461–8475.

Hampton, D.L., Heavner, M.J., Wescott, E.M., Sentman, D.D., 1996. Optical spectral characteristics of sprites. Geophysical Research Letters 23, 89–92.

Heavner, M.J., Sentman, D.D., Moudry, D.R., Wescott, E.M., Siefring, C.L., Morril, J.S., Bucsela, ., 2000. In: Siskind, D.E., Echerman, S.D., Summers, M.E. (Eds.), Sprites, Blue Jets, and Elves: Optical Evidence of Energy Transport Across the Stratopause, American Geophysical Union, Washington, DC, pp. 69–82.

Katayama, D., 1984. Collision induced electronic energy transfer between the $A^2\Pi_{ui}(v=4)$ and $X^2\Sigma_g^+(v=8)$ rotational manifolds of $N_2^+$. Journal of Chemical Physics 81, 3495–3499.

Katayama, D., Miller, T., Bondybey, V., 1980. Collisional deactivation of selectively excited $N_2^+$. Journal of Chemical Physics 72, 5469–5475.

Krupenie, P.H., 1972. The spectrum of molecular oxygen. Journal of Physical and Chemical Reference Data 1, 423–534.

Lyons, W.A., 1994. Characteristics of luminous structures in the stratosphere above thunderstorms as imaged by low-light video. Geophysical Research Letters 21, 875–878.

Mende, S.B., Rairden, R.L., Swenson, G.R., Lyons, W.A., 1995. Sprite spectra: $N_2$ 1PG band identification. Geophysical Research Letters 22, 2633–2636.

Milikh, G., Valdivia, J.A., Papadopoulos, K., 1998. Spectrum of red sprites. Journal of Atmospheric and Solar-Terrestrial Physics 60, 811–829.

Morrill, J.S., Benesch, W.M., 1994. Role of $N_2(A_5'\Sigma_g^+)$ in the enhancement of $N_2B^3\Pi_g(v=10)$ populations in the afterglow. Journal of Chemical Physics 101, 6529–6537.

Morrill, J.S., Benesch, W.M., 1996. Auroral $N_2$ emissions and the effect of collisional processes on $N_2$ triplet state vibrational populations. Journal of Geophysical Research 101, 261–274.

Morrill, J.S., Bucsela, E.J., Pasko, V.P., Berg, S.L., Heavner, M.J., Moudry, D.R., Benesch, W.M., Wescott, E.M., Sentman, D.D., 1998. Time resolved $N_2$ triplet state vibrational populations and emissions associated with red sprites. Journal of Atmospheric and Solar-Terrestrial Physics 60, 811–829.

Morrill, J.S., Bucsela, E.J., Siefring, C.L., Heavner, M.J., Berg, S.L., Moudry, D.R., Slinker, S., Fernsler, R., Wescott, E.M., Sentman, D.D., Osborne, D., 2002. Electron energy and electric field estimates in sprites derived from ionized and neutral $N_2$ emissions. Geophysical Research Letters 29, 100-1 to 100-4.

Pasko, V.P., Inan, U.S., Taranenko, Y.N., Bell, T.F., 1995. Heating, ionization and upward discharges in the mesosphere due to intense quasi-electrostatic thundercloud fields. Geophysical Research Letters 22, 365–368.

Pasko, V.P., Inan, U.S., Bell, T.F., Taranenko, Y.N., 1997. Sprites produced by quasi-electrostatic heating and ionization in the lower ionosphere. Journal of Geophysical Research 102, 4529–4561.

Pearse, R.W.B., Gaydon, A.G., 1976. The Identification of Molecular Spectra, 4th Edition. Chapman and Hall, London.

Picard, R.H., Inan, U.S., Pasko, V.P., Winick, J.R., Wintersteiner, P.P., 1997. Infrared glow above thunderstorms. Geophysical Research Letters 24, 2635–2638.

Piper, L.G., 1989. The excitation of $N_2(B^3\Pi_g,\ v=1-12)$ in the reaction between $N_2(A^3\Pi_g, v=1-12)$ and $N_2(X, v\geqslant 5)$. Journal of Chemical Physics 91, 864–873.

Piper, L., Green, B.D., Blumberg, W.A.M., Wolnik, S., 1985. $N_2^+$ Meinel band quenching. Journal of Chemical Physics 82, 3139–3145.

Rowland, H.L., 1998. Theories and simulations of elves, sprites, and blue jets. Journal of Atmospheric and Solar-Terrestrial Physics 60, 831–844.

Sentman, ., Wescott, E.M., 1993. Observations of upper atmospheric optical flashes recorded from an aircraft. Geophysical Research Letters 20, 2857–2860.

Sentman, D.D.P.I., et al., 1997. Energetics of upper atmospheric excitation by lightning (EXL), 1998. NASA Grant NAG5-5019.

Siefring, C.L., Morril, J.S., Bucsela, E.J., Pasko, V.P., Berg, S.L., Benesch, W.M., Wescott, E.M., Heavner, M.J., 1997. Predicted near-UV spectroscopy of sprites. EOS Transactions 78, F83.

Suszcynsky, D.M., Roussel-Dupre, R., Lyons, W.A., Armstrong, R.A., 1998. Blue-light imagery and photometry of sprites. Journal of Atmospheric and Solar-Terrestrial Physics 60, 801–809.

Vallance Jones, A., 1974. Aurora, Geophysics and Astrophysics Monographs. D. Reidel, Hingham, MA, USA.